Structural Reorganizations accompanying the Nickel(II)–Nickel(I) Redox change in Nickel Complexes with the Tripodal Ligand $MeC(CH_2PPh_2)_3$(Triphos, L). *X*-Ray Crystal Structure of $[NiL(I)]_2[As_6I_8]$ *

Piero Zanello and Arnaldo Cinquantini
Dipartimento di Chimica dell' Università di Siena, Pian dei Mantellini, 44-53100 Siena, Italy
Carlo A. Ghilardi, Stefano Midollini, Simonetta Moneti, and Annabella Orlandini
Istituto per lo Studio della Stereochimica ed Energetica dei Composti di Coordinazione, CNR Via J. Nardi, 39-50132 Firenze, Italy
Alessandro Bencini
Dipartimento di Chimica, Università di Firenze, Via Maragliano, 77-50144 Firenze, Italy

The stereodynamic aspects of the nickel(II)–nickel(I) conversion in complexes of the tridentate phosphine $MeC(CH_2PPh_2)_3$, (triphos, L) have been analysed. The structural reorganization, which accompanies the redox change, is pointed out. The substantial electrochemical reversibility observed for the nickel(II)–nickel(I) reduction, being indicative of minor molecular rearrangement, is consistent with the simple elongation of the Ni–I bond distance in the nickel(I) with respect to the nickel(II) derivative [2.546(2) *vs.* 2.414(4) Å]. The nickel(II) complexes [NiL(X)]Y (X = Cl, Br, or I, Y = ClO_4) and $[NiL(I)]_2[As_6I_8]$ have been synthetized and characterized. A complete *X*-ray analysis has been carried out for $[NiL(I)]_2[As_6I_8]$. a = 22.500(8), b = 19.092(5), c = 24.912(12) Å, β = 109.29(4)°, space group *C*2/*c*, Z = 4. The *X*-ray results showed two very interesting features: the isolation of a tetrahedral nickel(II) complex with the unprecedented P_3X donor atom set and the formation of the new polyanionic cluster species $[As_6I_8]^{2-}$. An angular overlap model analysis was performed to rationalize the electronic spectra of the $[NiL(X)]^+$ complexes (X = Cl, Br, or I).

The chemical reversibility of the nickel(II)–nickel(I) redox change is rather common in co-ordination compounds. Many electrochemical investigations have dealt with the one-electron reduction of cyclic[1–11] or open-chain[1,7,8] tetra-aza- and cyclic[12] or open-chain[13] penta-aza-nickel(II) complexes. Metal-centred one-electron reductions have been also reported for nickel(II) complexes displaying NiN_2O_2[14,15] and NiS_4[16,17] co-ordinations. Finally, attention has been paid to phosphine complexes of nickel(II). Monodentate phosphines of low steric hindrance (PEt_3, PEt_2Ph),[18] bidentate ($Ph_2PCH_2CH_2PPh_2$),[17–20] tridentate $[PhP(CH_2CH_2PPh_2)_2]$, and tetradentate $[P(CH_2CH_2PPh_2)_3]$[20] phosphines have shown to be able to give reversible nickel(II)–nickel(I) couples, as, on the other hand, a variety of mixed-ligand systems do ($Ph_2PCH_2CH_2PPh_2$–dithiocarbamates,[17] $Ph_2PCH_2CH_2PPh_2$–dithiolates or –catecholates,[21] $Ph_2PCH_2CH_2PPh_2$–4,5-dimercapto-1,3-dithia-2-thione,[22] macrocycles having phosphorus and sulphur donor sets[23]). With relatively few exceptions [interlocked tetra-aza macrocycles,[8] $Ph_2PCH_2CH_2PPh_2$,[17–20] PEt_3 and PEt_2Ph,[18] $PhP(CH_2CH_2PPh_2)_2$ and $P(CH_2CH_2PPh_2)_3$,[20] and mixed phosphine–dithiocarbamates[17]], access to nickel(I) is rather difficult.

In order to complete a previous investigation dealing with the structural reorganizations accompanying the nickel(II)–nickel(I) conversion in nickel(II) complexes with tripodal tetradentate polyphosphines, which displayed an easy nickel(II)–nickel(I) reduction,[24] we analyse here the stereodynamic aspects of this conversion in complexes of the tridentate phosphine $MeC(CH_2PPh_2)_3$ (triphos). It has been reported for years that nickel(II) halides in the presence of L = triphos can easily be reduced to yield the pseudo-tetrahedral species NiL(X).[25] In the case X = I the reduction occurs without the addition of any external reducing agent. Indeed the only nickel(II) halide complexes of this ligand so far reported are the square-planar $[NiLX_2]$ (X = Cl or Br) complexes in which triphos acts as a bidentate ligand.[26]

Now we report the synthesis and characterization of the series [NiL(X)]Y (X = Cl, Br, or I, Y = ClO_4; X = I, Y = As_6I_8). A complete *X*-ray determination has been carried out for $[NiL(I)]_2[As_6I_8]$ compound, a preliminary communication of which has been already published.[27]

Results and Discussion

Synthesis and Properties of the Nickel(II) *Complexes* [NiL(X)]Y (X = Cl, Br, or I; Y = ClO_4) *and* $[NiL(I)]_2[As_6I_8]$.—The complex $[NiL(I)]^+$ was accidentally isolated as the cation in a salt of the arsenic–iodine cluster $[As_6I_8]^{2-}$, obtained by reaction of $Ni(ClO_4)_2 \cdot 6H_2O$ and triphos with AsI_3. This finding induced us to try the synthesis of the complexes $[NiL(X)]^+$ (X = Cl, Br, or I) by a simpler pathway. This was accomplished by the reaction of $Ni(ClO_4) \cdot 6H_2O$ with equimolar amounts of triphos and NBu_4X (X = Cl, Br, or I). The reaction of $NiCl_2$ with triphos affords the previously reported orange complex $[NiLCl_2]$.[26] Although a five-co-ordinate square-pyramidal geometry has been tentatively assigned to this compound on the basis of electronic spectra, we have found that the complex is definitely square planar with triphos acting as a bidentate ligand. Indeed the ^{31}P-{^1H} n.m.r. spectrum (CD_2Cl_2) at −60 °C shows two singlets at δ 12.1 (2 P) and −31.3 (1 P) which broaden on raising the temperature, thus indicating a rapid intramolecular exchange of unco-ordinated

---

* Bis{iodo[1,1,1-tris(diphenylphosphinomethyl)ethane-$\kappa^3 P,P',P''$]-nickel(II)} di-μ_3-iodo-hexakis(iodoarsenate).

Supplementary data available: see Instructions for Authors, *J. Chem. Soc., Dalton Trans.*, 1990, Issue 1, pp. xix—xxii.

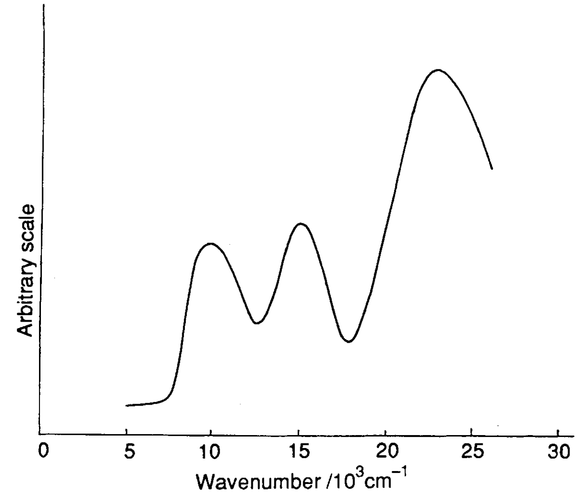

Figure 1. Reflectance spectrum of $[NiL(I)]_2[As_6I_8]$

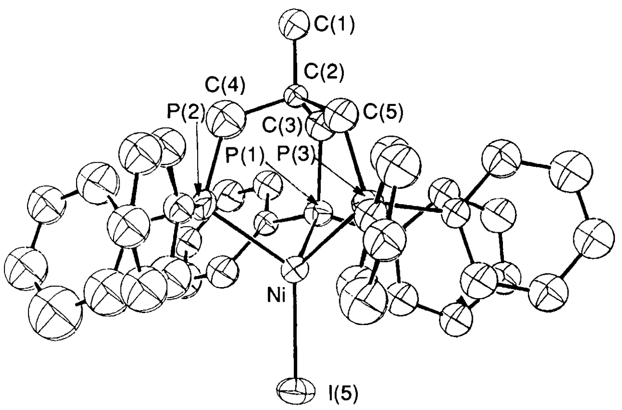

Figure 2. Perspective view of the complex cation $[NiL(I)]^+$. ORTEP drawing with 30% probability ellipsoids

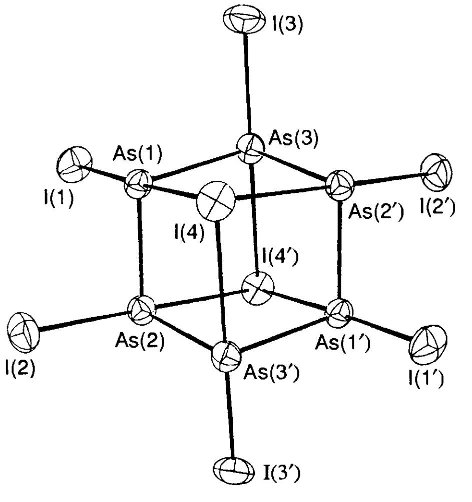

Figure 3. Perspective view of the cluster anion $[As_6I_8]^{2-}$. ORTEP drawing with 30% probability ellipsoids

and co-ordinated phosphorus atoms. If $NaBPh_4$ is added to the solution of $[NiLCl_2]$ in the place of $NBu^n{}_4ClO_4$, with gentle heating, the formation of the nickel(I) complexes [NiL(X)] occurs. The peculiarity of this reaction likely accounts for the failure of [NiL(X)] synthesis in spite of the many investigations, in our institute and elsewhere, of the reactivity of the nickel–triphos system.

Table 1. Selected bond distances (Å) and angles (°) for $[NiL(I)]_2[As_6I_8]$

As(1)–As(2)	2.450(5)	As(2)–I(2)	2.714(4)
As(1)–As(3)	2.463(5)	As(2)–I(4′)	3.051(4)
As(1)–I(1)	2.690(4)	As(3)–I(3)	2.659(4)
As(1)–I(4)	3.077(4)	As(3)–I(4′)	3.166(4)
As(2)–As(1)–As(3)	100.7(2)	I(2)–As(2)–I(4′)	179.0(3)
As(2)–As(1)–I(1)	89.8(1)	As(1)–As(3)–As(2′)	99.1(1)
As(2)–As(1)–I(4)	93.2(1)	As(1)–As(3)–I(3)	89.7(1)
As(3)–As(1)–I(1)	91.7(1)	As(1)–As(3)–I(4′)	89.5(1)
As(3)–As(1)–I(4)	90.7(1)	As(2′)–As(3)–I(3)	88.0(1)
I(1)–As(1)–I(4)	175.8(3)	As(2′)–As(3)–I(4′)	90.9(1)
As(1)–As(2)–As(3′)	99.7(1)	I(3)–As(3)–I(4′)	178.6(4)
As(1)–As(2)–I(2)	88.0(1)	As(1)–I(4)–As(2′)	75.4(1)
As(1)–As(2)–I(4′)	92.5(1)	As(1)–I(4)–As(3′)	73.9(1)
As(3′)–As(2)–I(2)	89.4(1)	As(2′)–I(4)–As(3′)	74.9(1)
As(3′)–As(2)–I(4′)	91.4(1)		
Ni–P(1)	2.240(9)	Ni–P(3)	2.248(9)
Ni–P(2)	2.244(9)	Ni–I(5)	2.414(4)
P(1)–Ni–P(2)	94.1(3)	P(2)–Ni–P(3)	92.7(4)
P(1)–Ni–P(3)	91.6(3)	P(2)–Ni–I(5)	124.6(3)
P(1)–Ni–I(5)	121.0(3)	P(3)–Ni–I(5)	124.2(3)

The complexes are stable under an inert gas atmosphere; [NiL(X)]Y behave as 1:1 electrolytes, while $[NiL(I)]_2[As_6I_8]$ behaves as a 1:2 electrolyte in nitroethane solutions. The compounds are paramagnetic with effective magnetic moments in the range 2.91–3.04. The visible-u.v. spectra are essentially the same in the solid state and in solution (Figure 1) and are very similar to each other. Both the values of the effective magnetic moments and the observed electronic spectra appear peculiar in comparison with the corresponding ones for previously reported pseudo-tetrahedral nickel(II) complexes.[28] These findings deserve some further comment (see below).

Structural Features of the Species $[NiL(I)]^+$ *and* [NiL(X)]. *Description of the Structure of the Complex* $[NiL(I)]_2[As_6I_8]$.—The *X*-ray structure of the nickel(I) complex [NiL(I)] was presented some years ago.[25]

The molecular structure of the corresponding nickel(II) complex consists of $[NiL(I)]^+$ cations and $[As_6I_8]^{2-}$ cluster anions, perspective views of which are given in Figures 2 and 3 respectively. Selected bond distances and angles are reported in Table 1. The *X*-ray results have shown two very interesting points: the isolation of a tetrahedral nickel(II) complex with the unprecedented P_3X donor atom set and the achievement of the new polyanionic cluster species $[As_6I_8]^{2-}$.

In the complex cation the nickel atom displays a distorted-tetrahedral geometry being surrounded by the three phosphorus atoms of the triphos ligand and by an iodine atom. The values of the P–Ni–P [91.6(3)—94.1(3)°] as well as of the P–Ni–I [121.0(3)—124.6(3)°] bond angles well evidence the distortion from the ideal tetrahedral geometry due to the steric constraints of the triphos ligand.

Of interest is a comparison of the $[Ni^{II}L(I)]^+$ cation with the molecular unit $[Ni^{I}L(I)]$. While the Ni–P bond distances of the monopositive species are only slightly larger than those of the uncharged one [2.244(4) (av.) *vs.* 2.220(2) (av.) Å], the values of the Ni–I distances display a significant difference, being markedly shorter in the first [2.414(4) *vs.* 2.546(2) Å]. Both the triphos derivatives have an open-shell configuration with two unpaired electrons in the nickel(II) and one unpaired electron in the nickel(I) species (triplet and doublet states respectively). The

Table 2. Electrochemical features for the reduction process exhibited by $[\mathrm{NiL(X)}]^+$ (X = Cl, Br, or I)

Complex	$E^\circ(\mathrm{Ni^{II}\text{–}Ni^{I}})$/V	$D/\mathrm{cm^2\,s^{-1}}$	$E_\mathrm{p}(\mathrm{Ni^{I}\text{–}Ni^{0}})$/V *	Solvent
$[\mathrm{NiL(Cl)}]^+$	−0.15	3.2×10^{-6}	< −1.5	$\mathrm{CH_2Cl_2}$
	−0.25	2.8×10^{-6}	−1.03	MeCN
$[\mathrm{NiL(Br)}]^+$	−0.10	6.7×10^{-6}	< −1.5	$\mathrm{CH_2Cl_2}$
	−0.19	4.8×10^{-6}	−1.02	MeCN
$[\mathrm{NiL(I)}]^+$	−0.05	6.4×10^{-6}	−1.34	$\mathrm{CH_2Cl_2}$
	−0.09	4.8×10^{-6}	−0.97	MeCN

* Peak potential for irreversible process, measured at 0.2 V s^{-1}.

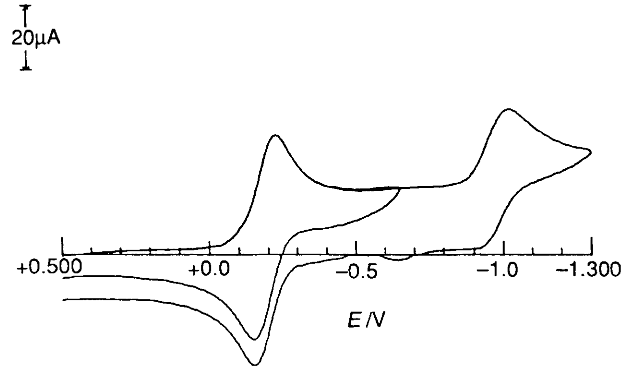

Figure 4. Cyclic voltammogram recorded at a platinum electrode of a deaerated MeCN solution containing $[\mathrm{NiL(Br)}]\mathrm{ClO_4}$ (1.54×10^{-3} mol dm^{-3}) and $\mathrm{NEt_4ClO_4}$ (0.1 mol dm^{-3}). Scan rate 0.5 V s^{-1}

frontier molecular orbital (responsible for the redox properties) is a degenerate *e* set, having metal d_π character, involved in antibonding interaction with the iodine p_π orbitals. This is consistent with the elongation of the Ni–I distance from the nickel(II) to the nickel(I) species. Moreover the larger distortion in the nickel(I) species (I–Ni–P 116.2—125.3°) with respect to the nickel(II) one (121.0—124.6°) could be attributed to the uneven occupation of the degenerate *e* set, which is responsible for a Jahn–Teller effect.

The cluster anion, an extensive description of which has been reported previously,[27] possesses crystallographic imposed C_i symmetry, with a distorted cubane-like structure. Six vertices of the cube are occupied by arsenic atoms and two diagonally opposite corners by two iodine atoms. Each arsenic atom completes its four-co-ordination by being additionally bound to a terminal iodine atom. Bond distances and angles are well in the range of values reported for a variety of polyarsenic species.[29]

Electrochemistry.—The redox propensity of the nickel(II) complexes $[\mathrm{NiL(X)}]^+$ can be deduced from the cyclic voltammetric response of $[\mathrm{NiL(Br)}]\mathrm{ClO_4}$ shown in Figure 4. Two reduction steps are displayed, the less cathodic one exhibiting a directly associated oxidation process in the reverse scan. Ill defined anodic processes are present at potentials higher than +1 V. In view of their chemical irreversibility as well as their difficult attribution [ligand-centred oxidation (triphos and/or halogen) or metal-centred oxidation nickel(II)–nickel(III)] we will disregard them.

Controlled-potential coulometric tests performed in correspondence to the first cathodic process ($E_\mathrm{w} = -0.5$ V) showed it to involve the consumption of one electron per molecule.

Analysis[30] of the relevant cyclic voltammetric response with scan rate v varying from 0.02 to 51.20 V s^{-1} indicates that: (*i*) the $i_{\mathrm{p_a}}/i_{\mathrm{p_c}}$ ratio is constantly equal to 1 : 1; (*ii*) the current function $i_{\mathrm{p_c}}v^{-\frac{1}{2}}$ is essentially constant; (*iii*) the difference between the forward and backward peak potentials ΔE_p progressively increases from 74 to 232 mV. Taking into account that, under the same experimental conditions, the one-electron oxidation of ferrocene exhibits a quite similar ΔE_p trend with scan rate, we consider these parameters as diagnostic for a simple, essentially reversible, one-electron reduction.

The peak height of the second cathodic step allows us to attribute it to the nickel(I)–nickel(0) reduction, whose electrochemical irreversibility testifies to a quick destruction of the starting molecular framework.

A qualitatively similar behaviour holds in a non-co-ordinating dichloromethane solution, except for the quasi-coalescence of the nickel(I)–nickel(0) step with a ligand-centred multielectron process. Table 2 summarizes the electrode potentials for the cited redox changes in the series $[\mathrm{NiL(X)}]^+$.

It should be noted that the potential E° ($\mathrm{Ni^{II}\text{–}Ni^{I}}$) becomes less negative in going from X = chloride to iodide, *i.e.* there is a linear correlation of the potential with the electrodonating ability of the halide substituents (I > Br > Cl); this is also expressed by the 'ligand constant' parameter P_L[31] (correlation coefficients: 1.0 in $\mathrm{CH_2Cl_2}$; 0.99 in MeCN). This observation seems to confirm the above hypothesis that the molecular orbital level accepting or releasing the electron is $M_{d_\pi}\text{–}X_{p_\pi}$ antibonding in nature or at least that the metal–halogen character is such as to govern the electrochemical trend.

The extent of reversibility of an electron transfer is related to the occurrence of more or less significant structural reorganizations accompanying the redox change.[32] The substantial electrochemical reversibility of the present nickel(II)–nickel(I) reductions, being indicative of minor molecular rearrangements, is in good accord with the simple elongation of the Ni–I bond distance found experimentally in the iodo-derivative.

Angular Overlap Model Analysis.—The observed electronic spectra of $[\mathrm{NiL(I)}]_2[\mathrm{As_6I_8}]$ show three bands at 10.0×10^3, 15.2×10^3, and 22.4×10^3 cm^{-1} attributable to *d–d* transitions. The electronic spectra of pseudo-tetrahedral nickel(II) complexes[32] are characterized by three main *d–d* bands, two bands arising from $^3F \longrightarrow {}^3F$ transitions in the ranges 4 000—7 000 and 7 000—11 000 cm^{-1} respectively; the third band is usually assigned to a $^3F \longrightarrow {}^3P$ transition in the range 15 000—20 000 cm^{-1}. It is apparent that the spectrum observed for the $[\mathrm{NiL(I)}]^+$ chromophore does not fall in the observed frequency range, all the observed transitions being at distinctly higher frequencies.

In order to rationalize the electronic spectra of the present chromophore we have applied the angular overlap model of the ligand field[33–35] in the simplest parametrization scheme which treats the bond between the ligand and the metal *d* orbitals using σ and π interactions.[35] Although some of the postulates which are at the basis of this model have been reformulated and a more sophisticated model suggested,[34] we prefer to use the simplest one since it requires the minimum number of parameters and has already been found to be a very useful tool to rationalize the spectromagnetic properties of a number of

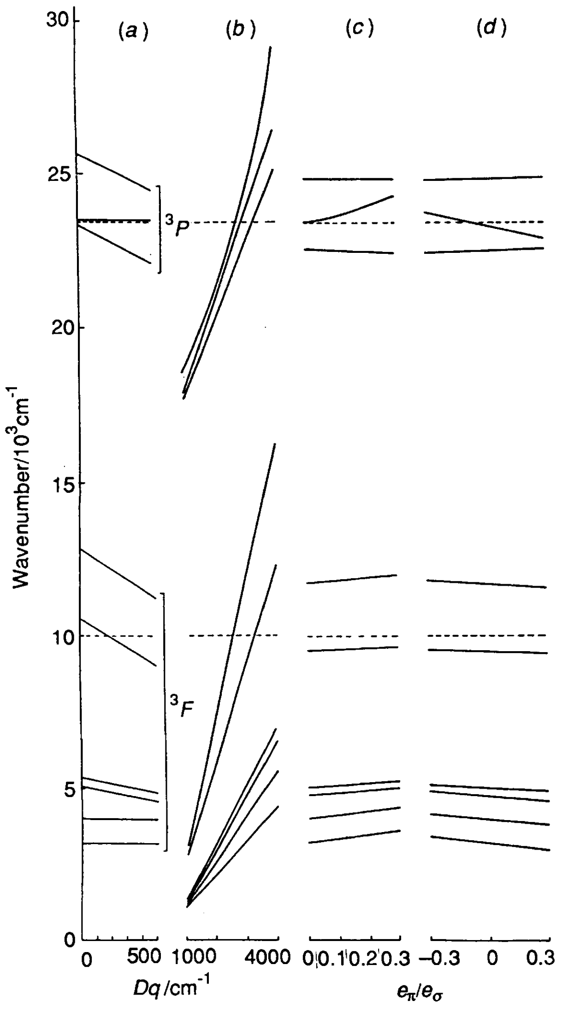

Figure 5. Computed electronic transitions for $[NiL(I)]_2[As_6I_8]$. The effects of varying: (*a*) Dq^I with $Dq^P = 3\,000$ cm^{-1}, $e_\pi{}^P/e_\sigma{}^P = 0.15$, $e_\pi{}^I = 0.0$ cm^{-1}; (*b*) Dq^P with $Dq^I = 350$ cm^{-1}, $e_\pi{}^I/e_\sigma{}^I = 0.10$, $e_\pi{}^P/e_\sigma{}^P = 0.15$; (*c*) $e_\pi{}^I/e_\sigma{}^I$ with $Dq^I = 350$ cm^{-1}, $Dq^P = 3\,000$ cm^{-1}, $e_\pi{}^P/e_\sigma{}^P = 0.15$; (*d*) $e_\pi{}^P/e_\sigma{}^P$ with $Dq^I = 350$ cm^{-1}, $e_\pi{}^I/e_\sigma{}^I = 0.10$, $Dq^P = 3\,000$ cm^{-1}. Dashed lines represent the experimental transition

transition-metal complexes.[35] Since in any case the number of parameters (e_σ and e_π for each atom ligand) is larger than the observables, we do not look for a best fit of the electronic spectrum, but report electronic transitions computed by varying the parameters over a wide range of values. The results of the calculations are shown in Figure 5.

In Figure 5(*a*) and (*b*) the effects of varying the Dq^I and Dq^P ($Dq = 3e_\sigma - 4e_\pi$) values are shown. The effect of the π interactions are shown in Figure 5(*c*) and (*d*) by varying the $e_\pi{}^I/e_\sigma{}^I$ and $e_\pi{}^P/e_\sigma{}^P$ ratios respectively. It is apparent that the larger effect on the electronic energies is played by the σ interaction with the P atoms of the triphos ligand. A reasonable agreement with experiment is obtained only by using $Dq^P = 3\,400$ cm^{-1}. Fixing Dq^I and the e_π/e_σ ratios at the values generally found in the literature,[35] namely $Dq^I = 350$ cm^{-1}, $e_\pi{}^I/e_\sigma{}^I = 0.1$, and $e_\pi{}^P/e_\sigma{}^P = -0.20$, a reasonable fit of the electronic transitions was obtained for $Dq^P = 3\,250$ cm^{-1}. The computed values are $<5.6 \times 10^3$, 10.3×10^3, 13.0×10^3, 23.1×10^3, and $>24.2 \times 10^3$ cm^{-1}. This Dq^P value is slightly larger than those observed in nickel phosphine systems which range between 1 900 and 2 300 cm^{-1}.

Using the same parameters a magnetic moment of 3.1 was computed using a 70% reduction of the spin–orbit coupling constant from the single-ion value to account for covalancy.

These calculations show that the ligand-field strength and the covalency of triphos towards nickel(II) is higher than those of monodentate phosphine ligands.

Experimental

All reactions were performed under dry nitrogen, using standard Schlenk techniques. The complex $[NiLCl_2]$ was prepared as previously described.[26] Its $^{31}P-\{^1H\}$ n.m.r. spectrum was recorded by a Varian VXR-300 spectrometer, operating at 121.421 MHz, relative to external phosphoric acid. Positive chemical shifts are downfield.

Synthesis of the Nickel(II) *Complexes* [NiL(X)]Y.—$[NiL(I)]_2[As_6I_8]$. To a solution of $Ni(ClO_4)_2 \cdot 6H_2O$ (0.5 mmol, 135 mg) in tetrahydrofuran (thf) (15 cm^3) the solid triphos ligand (0.5 mmol, 315 mg) was added at room temperature. Arsenic triiodide (1.5 mmol, 685 mg) in thf (20 cm^3) was added. Brown crystals of the complex were obtained by adding BuOH (20 cm^3). The crystals were filtered off and dried, yield 385 mg (50%) (Found: C, 32.30; H, 2.60; I, 37.75; Ni, 3.45. Calc. for $C_{82}H_{78}As_6I_{10}Ni_2P_6$: C, 31.90; H, 2.55; I, 41.15; Ni, 3.80%). $\mu_{eff.} = 3.04$.*

$[NiL(Cl)]ClO_4$. The salt $Ni(ClO_4)_2 \cdot 6H_2O$ (0.5 mmol, 133 mg) in thf (20 cm^3) was added to the stoicheiometric amount of triphos (0.5 mmol, 315 mg). Solid NBu_4Cl (0.5 mmol, 140 mg) was added. After addition of EtOH (5 cm^3) the solution was concentrated until crystallization began. The compound was filtered off and dried, yield 370 mg (91%) (Found: C, 61.20; H, 4.90. Calc. for $C_{41}H_{39}Cl_2NiO_4P_3$: C, 60.25; H, 4.80%), $\mu_{eff.} = 2.97$.

$[NiL(X)]ClO_4$ (X = Br *or* I). The compounds were prepared analogously to the chlorine derivative using NBu_4Br or NBu_4I instead of NBu_4Cl, yields 380 (89) and 395 mg (87%) (Found: C, 54.95; H, 4.70. Calc. for $C_{41}H_{39}BrClNiO_4P_3$: C, 57.10; H, 4.55. Found: C, 52.05; H, 4.40; Ni, 5.70. Calc. for $C_{41}H_{39}ClINiO_4P_3$: C, 54.10; H, 4.30; Ni, 6.45%). $\mu_{eff.} = 3.02$ (X = Br) and 2.91 (X = I).

Crystallography.—Crystal data for $[NiL(I)]_2[As_6I_8]$. $M = 3\,085.37$, monoclinic, space group $C2/c$, $a = 22.500(8)$, $b = 19.092(5)$, $c = 24.912(12)$ Å, $\beta = 109.29(4)°$, $U = 10\,100.6$ Å^3, $Z = 4$, $D_c = 2.028$ g cm^{-3}, $\lambda = 0.7107$ Å, μ(Mo-K_α) = 54.8 cm^{-1}, $F(000) = 5\,776$.

Enraf-Nonius CAD4 automatic diffractometer, brown parallelepiped crystal of dimensions *ca.* 0.10 × 0.15 × 0.50 mm, cell constants from 20 randomly selected reflections, $\bar{\omega}$–2θ mode with a scan speed of 8.24° min^{-1} and a scan width = $0.8 + 0.34 \tan\theta$, $2.5 < \theta < 20°$, graphite-monochromated Mo-K_α radiation, background measurements equal to half the scan time, three standard reflections periodically measured to check the stability of the crystal, standard deviations $\sigma(I)$ calculated according to ref. 36. Of a total of 5 175, 2 161 reflections having $I > 3\sigma(I)$ were considered observed. The intensities were corrected for Lorentz-polarization effects and for absorption.[37]

Solution and refinement of the structure. All the calculations were carried out on a SEL 32/77 computer, by using the SHELX 76[38] and ORTEP[39] programs. Atomic scattering factors were taken from ref. 40 for non-hydrogen atoms and from ref. 41 for the hydrogen atoms. Both the $\Delta f'$ and $\Delta f''$ components of the anomalous dispersion were included for the non-hydrogen atoms.[42] The function minimized during the least-squares refinement was $\Sigma w(|F_o| - |F_c|)^2$, the weights being defined as

---

* In ref. 27 a $\mu_{eff.}$ value of 3.25 was erroneously reported.

Table 3. Final positional parameters (× 10^4)

Atom	x	y	z
As(1)	−557(2)	404(2)	526(1)
As(2)	−64(2)	−757(2)	671(1)
As(3)	267(1)	1 102(2)	325(1)
I(1)	−57(1)	658(1)	1 648(1)
I(2)	−1 199(1)	−1 297(1)	617(1)
I(3)	−553(1)	2 139(1)	−55(1)
I(4)	−1 220(1)	159(1)	−754(1)
I(5)	−4 396(1)	−1 246(2)	−3 711(1)
Ni	−3 448(2)	−574(2)	−3 281(2)
P(1)	−2 947(4)	−57(5)	−3 817(3)
P(2)	−3 382(4)	368(5)	−2 725(4)
P(3)	−2 543(4)	−1 025(4)	−2 697(3)
C(1)	−1 519(13)	822(17)	−2 470(13)
C(2)	−2 077(12)	402(14)	−2 714(11)
C(3)	−2 201(14)	326(17)	−3 330(12)
C(4)	−2 610(16)	753(21)	−2 598(16)
C(5)	−2 004(15)	−302(16)	−2 456(14)
C(11)	−2 750(7)	−662(12)	−4 288(10)
C(21)	−3 257(7)	−1 031(12)	−4 655(10)
C(31)	−3 157(7)	−1 521(12)	−5 031(10)
C(41)	−2 549(7)	−1 643(12)	−5 040(10)
C(51)	−2 041(7)	−1 275(12)	−4 673(10)
C(61)	−2 142(7)	−784(12)	−4 297(10)
C(12)	−3 350(7)	622(12)	−4 282(9)
C(22)	−3 051(7)	1 079(12)	−4 547(9)
C(32)	−3 396(7)	1 605(12)	−4 904(9)
C(42)	−4 039(7)	1 673(12)	−4 997(9)
C(52)	−4 338(7)	1 215(12)	−4 732(9)
C(62)	−3 994(7)	690(12)	−4 374(9)
C(13)	−3 957(17)	1 052(13)	−3 023(13)
C(23)	−4 583(17)	833(13)	−3 187(13)
C(33)	−5 067(17)	1 311(13)	−3 430(13)
C(43)	−4 924(17)	2 006(13)	−3 509(13)
C(53)	−4 298(17)	2 225(13)	−3 344(13)
C(63)	−3 814(17)	1 747(13)	−3 101(13)
C(14)	−3 445(10)	109(13)	−2 049(9)
C(24)	−3 974(10)	−290(13)	−2 078(9)
C(34)	−4 085(10)	−484(13)	−1 580(9)
C(44)	−3 667(10)	−280(13)	−1 052(9)
C(54)	−3 137(10)	119(13)	−1 024(9)
C(64)	−3 026(10)	313(13)	−1 522(9)
C(15)	−2 585(10)	−1 486(14)	−2 076(9)
C(25)	−3 135(10)	−1 839(14)	−2 096(9)
C(35)	−3 159(10)	−2 218(14)	−1 625(9)
C(45)	−2 633(10)	−2 246(14)	−1 134(9)
C(55)	−2 083(10)	−1 893(14)	−1 114(9)
C(65)	−2 059(10)	−1 514(14)	−1 585(9)
C(16)	−2 206(8)	−1 668(13)	−3 025(10)
C(26)	−2 611(8)	−2 192(13)	−3 328(10)
C(36)	−2 375(8)	−2 752(13)	−3 555(10)
C(46)	−1 733(8)	−2 790(13)	−3 479(10)
C(56)	−1 328(8)	−2 266(13)	−3 176(10)
C(66)	−1 564(8)	−1 706(13)	−2 949(10)

$w = 1/\sigma^2(F_o)$. The structure was solved by the heavy-atom method, through Patterson and Fourier syntheses. The refinement was carried out by full-matrix least-squares cycles, the arsenic, iodine, nickel, and phosphorus atoms being assigned anisotropic thermal parameters. During the refinement the phenyl rings were treated as rigid bodies of D_{6h} symmetry with C–C 1.395 Å. Hydrogen atoms introduced in their geometrical positions were not refined. At convergence the R and R' factors were 0.053 and 0.052 respectively. Final positional parameters are given in Table 3.

Electrochemistry.—The materials and apparatus for electrochemistry have been described elsewhere.[43] The diffusion coefficients were calculated as previously described.[24] The potentials are referred to the aqueous calomel electrode. Under the present experimental conditions, the ferrocenium–ferrocene couple was located at $E^{\circ} = +0.38$ V in acetonitrile and at $E^{\circ} = +0.49$ V in dichloromethane solutions.

Acknowledgements

Thanks are due to Mr. F. Cecconi for technical assistance.

References

1 D. C. Olson and J. Vasilevskis, *Inorg. Chem.*, 1969, **8**, 1611.
2 F. V. Lovecchio, E. S. Gore, and D. H. Busch, *J. Am. Chem. Soc.*, 1974, **96**, 3109.
3 J. Y. Becher, J. B. Kerr, D. Pletcher, and R. Rosas, *J. Electroanal. Chem., Interfacial Electrochem.*, 1981, **117**, 87 and refs. therein.
4 R. R. Gagnè and D. M. Ingle, *Inorg. Chem.*, 1981, **20**, 420 and refs. therein.
5 N. Jubran, D. Meyerstein, and H. Cohen, *Inorg. Chim. Acta*, 1986, **117**, 129 and refs. therein.
6 M. Ciampolini, L. Fabbrizzi, M. Licchelli, A. Perotti, F. Pezzini, and A. Poggi, *Inorg. Chem.*, 1986, **25**, 4131 and refs. therein.
7 M. P. Suh, W. Shin, H. Kim, and C. H. Koo, *Inorg. Chem.*, 1987, **26**, 1846.
8 C. O. D. Bucheker and J. P. Sauvage, *Chem. Rev.*, 1987, **87**, 795 and refs. therein.
9 A. M. Stolzemberg and M. T. Stershic, *J. Am. Chem. Soc.*, 1988, **110**, 6391 and refs. therein.
10 P. W. Bernhardt, G. A. Lawrance, and D. F. Sangster, *Inorg. Chem.*, 1988, **27**, 4055.
11 D. Lexa, M. Momenteau, J. Mispelter, and J. M. Saveant, *Inorg. Chem.*, 1989, **28**, 30.
12 E. C. Constable, J. Lewis, M. C. Liptrot, P. R. Raithby, and M. Schroder, *Polyhedron*, 1983, **2**, 301 and refs. therein.
13 E. C. Constable, J. Lewis, and M. Schroder, *Polyhedron*, 1982, **1**, 311.
14 C. Gosden, K. P. Healy, and D. Pletcher, *J. Chem. Soc., Dalton Trans.*, 1978, 972.
15 G. Cros, J. P. Costes, and D. de Montauzon, *Polyhedron*, 1984, **3**, 585.
16 W. E. Geiger, jun., C. S. Allen, T. E. Mines, and F. C. Senftleber, *Inorg. Chem.*, 1977, **16**, 2003.
17 G. A. Bowmaker, P. D. W. Boyd, G. K. Campbell, J. M. Hope, and R. L. Martin, *Inorg. Chem.*, 1982, **21**, 1152.
18 G. Bontempelli, F. Magno, G. Schiavon, and B. Corain, *Inorg. Chem.*, 1981, **20**, 2579.
19 M. Martelli, G. Pilloni, G. Zotti, and S. Daolio, *Inorg. Chim. Acta*, 1974, **11**, 155.
20 D. L. DuBois and A. Miedaner, *Inorg. Chem.*, 1986, **25**, 4642.
21 G. A. Bowmaker, P. D. W. Boyd, and G. K. Campbell, *Inorg. Chem.*, 1982, **21**, 2403.
22 R. Vicente, J. Ribas, X. Solans, M. F. Altaba, A. Mari, P. De Loth, and P. Cassoux, *Inorg. Chim. Acta*, 1987, **132**, 229.
23 E. P. Kyba, R. E. Davis, M. A. Fox, C. N. Clubb, S. T. Liu, G. A. Reitz, V. J. Scheuler, and R. P. Kashyap, *Inorg. Chem.*, 1987, **26**, 1647.
24 C. A. Ghilardi, C. Mealli, S. Midollini, A. Orlandini, D. M. Proserpio, A. Cinquantini, and P. Zanello, *Struct. Chem.*, 1990, **1**, in the press.
25 P. Dapporto, G. Fallani, and L. Sacconi, *Inorg. Chem.*, 1974, **13**, 2847.
26 R. Davis and J. E. Fergusson, *Inorg. Chim. Acta*, 1970, **4**, 23.
27 C. A. Ghilardi, S. Midollini, S. Moneti, and A. Orlandini, *J. Chem. Soc., Chem. Commun.*, 1988, 1241.
28 L. Sacconi, F. Mani, and A. Bencini, 'Comprehensive Coordination Chemistry,' eds. G. Wilkinson, R. D. Gillard, and J. A. McCleverty, Pergamon, Oxford, 1987, vol. 5, p. 1.
29 'Interatomic Distances,' *Chem. Soc. Spec. Publ.*, The Chemical Society, London, 1965, no. 18; H. J. Whitfield, *J. Chem. Soc. A*, 1970,

1800; *J. Chem Soc., Dalton Trans.*, 1973, 1737; W. Schmettow and H. G. von Schnering, *Angew. Chem., Int. Ed. Engl.*, 1977, **16**, 857; M. Di Vaira, S. Midollini, and L. Sacconi, *J. Am. Chem. Soc.*, 1979, **101**, 1757; C. H. E. Belin, *ibid.*, 1980, **102**, 6036; A. L. Rheingold and P. J. Sullivan, *Organometallics*, 1983, **2**, 327; R. C. Haushalter, B. W. Echhorn, A. L. Rheingold, and S. J. Geib, *J. Chem. Soc., Chem. Commun.*, 1988, 1027; O. J. Scherer, W. Wiedemann, and G. Wolmershauser, *J. Organomet. Chem.*, 1989, **C11**, 361.

30 E. R. Brown and J. R. Sandifer, in 'Physical Methods of Chemistry: Electrochemical Methods,' eds. B. W. Rossiter and J. F. Hamilton, Wiley, New York, 1986, vol. 2, ch. 4.

31 J. Chatt, C. T. Kan, G. J. Leigh, C. J. Pickett, and D. R. Stanley, *J. Chem. Soc., Dalton Trans.*, 1980, 2032.

32 W. E. Geiger, *Prog. Inorg. Chem.*, 1985, **33**, 275.

33 C. E. Schaffer, 'Wave Mechanics,' eds. W. C. Price, S. S. Chissick, and T. Ravensdale, Butterworths, London, 1973, p. 173.

34 M. Gerloch, J. H. Harding, and R. G. Wooly, *Struct. Bonding*, (*Berlin*), 1981, **46**, 1.

35 A. Bencini, C. Benelli, and D. Gatteschi, *Coord. Chem. Rev.*, 1984, **60**, 131.

36 P. W. R. Corfield, R. J. Doedens, and J. A. Ibers, *Inorg. Chem.*, 1976, **6**, 197.

37 N. Walker and D. Stuart, *Acta Crystallogr., Sect. A*, 1983, **39**, 158.

38 G. M. Sheldrick, SHELX System of Computing Programs, University of Cambridge, Cambridge, 1976.

39 C. K. Johnson, Report ORNL-5138, Oak Ridge National Laboratory, Tennessee, 1976.

40 'International Tables for *X*-Ray Crystallography,' Kynoch Press, Birmingham, 1974, vol. 4, p. 99.

41 R. F. Stewart, E. R. Davidson, and W. T. Simpson, *J. Chem. Phys.*, 1965, **42**, 3175.

42 Ref. 40, p. 149.

43 M. Gullotti, L. Casella, A. Pintar, E. Suardi, P. Zanello, and S. Mangani, *J. Chem. Soc., Dalton Trans.*, 1989, 1979.

Received 21*st May* 1990; *Paper* 0/02231D